Available online at www.sciencedirect.com

ScienceDirect

Procedia Computer Science 100 (2016) 1121 – 1126

Procedia Computer Science

Conference on ENTERprise Information Systems / International Conference on Project MANagement / Conference on Health and Social Care Information Systems and Technologies, CENTERIS / ProjMAN / HCist 2016, October 5-7, 2016

Deformation monitoring using Persistent Scatterer Interferometry and Sentinel-1 SAR data

Núria Devanthéry[a]*, Michele Crosetto[a], María Cuevas-González[a], Oriol Monserrat[a], Anna Barra[a], Bruno Crippa[b]

[a] *Centre Tecnològic de Telecomunicacions de Catalunya (CTTC), Division of Geomatics, Av. Gauss, 7, E-08860 Castelldefels (Barcelona), Spain*
[b]*Department of Earth Sciences, University of Milan, Via Cicognara 7, I-20129 Milan, Italy*

Abstract

During the last decades, Persistent Scatterer Interferometry (PSI) has demonstrated to be a powerful tool able to measure and monitor deformations. This technique makes use of large stacks of interferometric SAR images to derive the deformation maps and deformation time series. In this paper, Sentinel-1 images are used to derive the deformation monitoring over the Catalonia region (Spain). These images brings new improvements due to its wide coverage and high revisiting time, which allows us to make a wide area processing.

The first part of the paper describes the data processing implemented by the authors to analyze Sentinel-1 data and the PSI approach used in this ongoing research. The second part of the paper illustrates the results derived over an area of 6750 km^2 using Sentinel-1 images.

Peer-review under responsibility of the organizing committee of CENTERIS 2016

Keywords: PSI; DInSAR; deformation monitoring; Sentinel-1.

* Corresponding author. Tel.: +34 936 452 900; fax: +34 936 452 901.
E-mail address: ndevanthery@cttc.cat

Peer-review under responsibility of the organizing committee of CENTERIS 2016
doi:10.1016/j.procs.2016.09.263

1. Introduction

Persistent Scatterer Interferometry (PSI) is a group of Differential SAR Interferometry (DInSAR) techniques widely used to measure and monitor terrain deformations[1]. It uses large stacks of Synthetic Aperture Radar (SAR) images and suitable data modelling procedures that allow the estimation of different parameters. These parameters include the deformation time series, the average displacement rates and the so-called residual topographic error. It has been successfully used in a wide range of applications mainly related to the fields of urban, peri-urban and built[2,3,4,5], subsidence and uplift[6,7,8,9], landslides[10,11,12,13], and geophysics[14,15,16,17].

During the last two decades, PSI has experienced a major development. Several approaches to PSI techniques have been proposed[18,19,20,21,22,23]. This development is mainly related to the progress accomplished through the exploitation of C-band data from ERS-1/2, Envisat and Radarsat. The data acquired by these satellites covers long periods of time, a key aspect to guarantee a long-term deformation monitoring. The availability of X-band data resulted in new improvements due to the high sensitivity of this wavelength and the high resolution of the images. Thus, it allowed to generate a denser sampling of Persistent Scatterers (PSs), a higher sensitivity to small displacements and a remarkable quality improvement of the time series compared to the C-band[24,25]. A new significant improvement is expected to occur with the data acquired by the C-band sensor onboard the Sentinel-1 satellites. Sentinel-1A, launched on 3 April 2014, acquires interferometric C-band SAR data and offers an improved data acquisition capability with respect to previous C-band sensors (ERS-1/2, Envisat and Radarsat), increasing considerably the deformation monitoring potential. It acquires images covering 250 by 180 km with a revisiting cycle of 12 days in the Interferometric Wide Swath (IW) data acquisition mode, which will be reduced to 6 days when the images acquired by the Sentinel-1B satellite are available. The Sentinel-1 coverage might be essential for certain applications that might benefit from a wide-area PSI monitoring using C-band Sentinel-1 data. Moreover, this data allows an improvement of the coherence, mainly related to the high temporal sampling, which imply a reduced temporal decorrelation of the interferometric pair[26]. Finally, these data are free of charge, which represent an advantage with respect to X-band sensors such as TerraSAR-X data, which are expensive.

This research is focused on the application of Persistent Scatterer Interferometry (PSI) for terrain deformation detection and measurement over the region of Catalonia (Spain) using the SAR data acquired by the Sentinel-1 satellite of the European Space Agency.

2. Methodology

The methodology used in this work is a PSI technique, which exploits a 2+1D phase unwrapping using a set of redundant interferograms. A key aspect of the procedure is the interferometric processing of Sentinel-1 interferometric data.

In the IW mode, Sentinel-1 acquires data with a swath of 250 km using the TOPS (Terrain Observation by Progressive Scan) imaging mode. The Sentinel-1 data need extra processing with respect to the standard StripMap processing[27], due to the TOPS characteristics. As a consequence, due to a high Doppler rate caused by the azimuth antenna beam steering, the image co-registration step needs to be very accurate[28]. To achieve such an accuracy, a two-step process has been proposed by different authors[27,28,29]: first, a pixel level co-registration by using classical SAR image co-registration methods is carried out, e.g. using orbit information or cross-correlation methods, and then a refinement of the accuracy by using the Spectral Diversity[28,29] is done.

The PSI approach used in this study is a 2+1D phase unwrapping, which starts with a set of N images and a redundant net of M interferograms. The main processing steps[30] of the procedure are briefly described below:

- Atmospheric phase screen (APS) estimation and removal. A phase unwrapping is performed over the N-1 consecutive interferograms, multi-looked 10 in range and 2 in azimuth to reduce the noise and ease the phase unwrapping. A direct integration, which retrieve the images phases with respect to a given image, is then carried out over the unwrapped interferograms. Finally, the APS estimation is performed by means of a set of spatio-temporal filters[18,19,20,22] and removed from the original interferograms.
- Deformation velocity and residual topographic error (RTE) estimation. The deformation velocity and RTE are estimated over a set of PSs, from the M wrapped APS-free interferograms, using the periodogram method.

- RTE removal. The RTE phase component is removed from the wrapped APS-free interferograms. This is especially important when performing measurements in urban areas at full resolution to avoid confusing the deformation with other components, as well as to avoid phase unwrapping errors due to phase gradients related to RTE.
- 2+1D phase unwrapping. This is the key step of the procedure, where the accumulated deformation map and the time series are derived from the redundant network of interferograms free of APS and RTE. A spatial 2D phase unwrapping is performed interferogram wise using the Minimum Cost Flow method[30,31]. Then, a 1D phase unwrapping is performed pixel wise over the M interferograms. This last step is able to detect and correct the errors generated during the 2D phase unwrapping stage, and provides tools to control the quality of the derived time series. It uses an iterative LS procedure[33,34,35] which fully exploits the integer nature of the unwrapping errors. It is based on the estimation of the following system of equations:

$$\begin{matrix} \Delta\varphi_{MS} = \varphi_S - \varphi_M \\ \tilde{\varphi}_0 = 0 \end{matrix} \quad (1)$$

where $\Delta\varphi_{MS}$ is the unwrapped interferometric phase (the observation), *S* and *M* are the slave and master images and φ_S and φ_M are the corresponding unknown phases. The phase of the first image φ_0 is set to zero. The system is solved by means of an iterative LS driven by two key parameters: the residuals $\hat{\varphi}_{res}$ and the redundancy of the network.

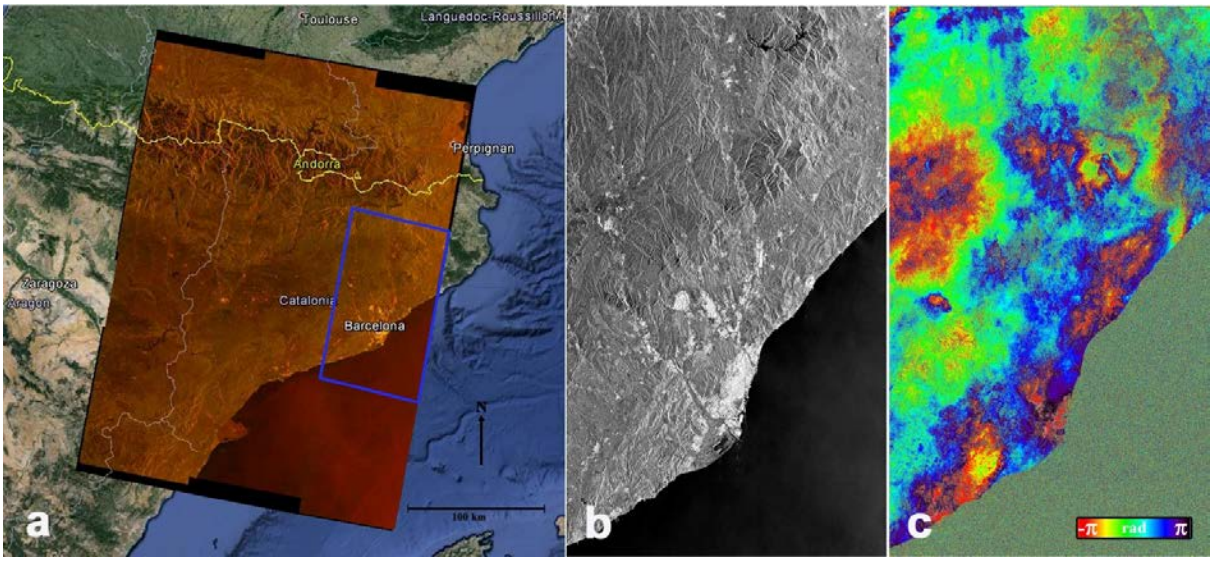

Fig. 1. (a) Amplitude of two merged IW Sentinel-1 scenes covering the region of Catalonia (Spain), superimposed to Google Earth. The blue rectangle shows the area processed; (b) Mean Amplitude of 24 IW Sentinel-1 images of the area shown in the blue rectangle, which comprises 6 bursts of the swath 1; (c) 12-day interferogram of the area of interest.

3. Results

The results described are part of an ongoing research with the aim to monitor the full region of Catalonia (Spain) using Sentinel-1 images. To cover the area of interest, more than one scene is required (see Fig. 1a). An IW mode Sentinel-1 scene is composed by 3 swaths, which are acquired by steering the beam in range, and 9 bursts each swath,

which are acquired by electronically steering the beam from backward to forward in the azimuth direction. The bursts are synchronized from pass to pass to ensure the alignment of interferometric pairs. In this study, the area of interest is covered by 26 bursts distributed in 3 swaths. This paper shows the results obtained over an area of approximately 6750 km^2, covered by 6 bursts in a single swath (see Fig. 1b and 1c).

The main PSI products are the accumulated deformation map and the time series of the deformation derived from a set of 24 IW SLC Sentinel-1 images, spanning the period from March 2015 to January 2016. A network of interferograms with perpendicular baselines ranging from -170 to 210 m was used. Fig. 2a shows the accumulated deformation map obtained with the direct integration of the consecutives interferograms. This procedure was performed over the interferograms multi-looked 5 in range and 1 in azimuth, i.e., with a footprint of approximately 14 x 20 m in range and azimuth, respectively. The figure shows a good coverage of PS over all the area of interest, and a good connection between all the urban areas (see Fig. 2b and 2c). Figure 2b shows the PS density over the city of Barcelona, which is 620 PS/km^2. This is a good density considering the resolution of the images.

Fig. 2a allows obtaining a comprehensive outlook of the deformation phenomena occurring in wide areas. In this case, most of the area is stable (in green). However, some important deformation phenomena have been identified. Areas in red show displacements away from the sensor, while the blue ones indicate displacements toward the SAR sensor. Note that these values refer to the SAR Line-of-Sight (LOS).

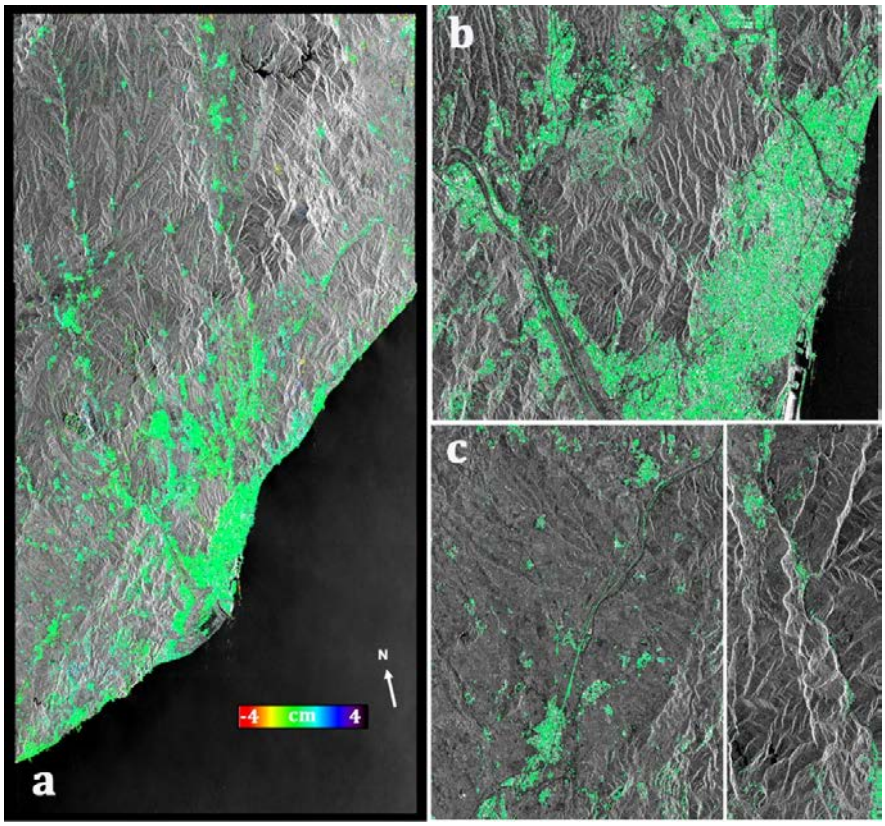

Fig. 2. (a) Accumulated deformation map in radar geometry superimposed to the Mean Amplitude. This map covers an area of 6750 km^2; (b) PS density in the city of Barcelona and metropolitan area; (c) PS coverage in highways and roads connecting urban areas.

Fig. 3 illustrates two examples of major deformation phenomena found in this study. Fig.3a illustrates a deformation near the village of Sallent, with two differentiated displacement rates: the area in yellow reach more than 3 cm in almost one year, while a higher displacement was estimated in the area in red. Fig 3b illustrates a subsidence up to 9 cm in a dump near Piera, in the metropolitan area of Barcelona.

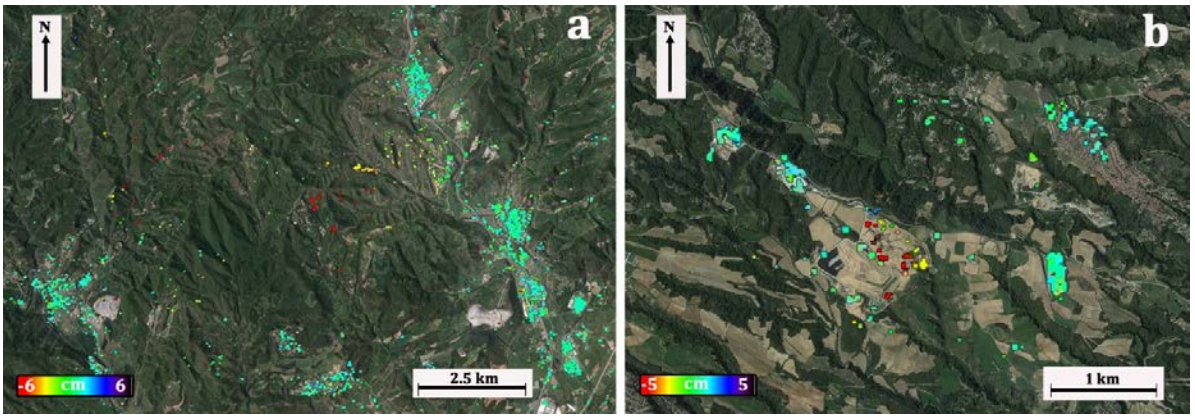

Fig. 3. (a) Accumulated deformation map over the area of Sallent geocoded to Google Earth; (b) Accumulated deformation map over a dump in Piera geocoded to Google Earth.

4. Conclusions

In this paper, the results achieved so far using Persistent Scatterer Interferometry and Sentinel-1 images have been shown. The interferometric procedure used by the authors to derive the deformation maps and time series from a stack of Interferometric Wide Sentinel-1 images has been described, which consists in a 2+1D phase unwrapping approach.

The deformation map derived over an area of 6750 km^2, a wide region in Catalonia (Spain), which comprises 6 bursts of a single swath, has been illustrated. The density of PS achieved in this study has proved to be good: 620 PS/km^2 in urban areas with a good coverage and connection between urban areas.

The next step of the procedure will be to perform the analysis for the 26 bursts into the 3 swaths of the IW Sentinel-1 scenes covering the entire region. The goal is to derive the deformation map over the region of Catalonia, performing local densification when required to study any given deformation phenomena.

Acknowledgements

This work has been partially funded by the Spanish Ministry of Economy and Competitiveness through the project MIDES “Monitorización y análisis sistemáticos de deformaciones del terreno, estructuras e infraestructuras sobre areas muy extensas” (Ref: CGL2013-43000-P).

References

1. Crosetto, M., Monserrat, O., Cuevas-González, M., Devanthéry, N. Persistent Scatterer Interferometry: a review. *ISPRS J. of Photogrammetry and Remote Sensing*, 2016. 115, 78-89.
2. Cigna, F., Osmanoglu, B., Cabral-Cano, E., Dixon, T.H., Ávila-Olivera, J.A., Garduño-Monroy, V.H., DeMets, C., Wdowinski, S. Monitoring land subsidence and its induced geological hazard with Synthetic Aperture Radar Interferometry: A case study in Morelia, Mexico, *Remote Sensing of Environment*, 2012. 117, 146–161.
3. Sousa, J.J., Bastos, L. Multi-temporal SAR interferometry reveals acceleration of bridge sinking before collapse. *Natural Hazards and Earth System Science*, 2013. 13(3), 659-667.
4. Wasowski, J., Bovenga, F., Refice, A., Nitti, D., Nutricato, R. High Resolution PSI for Mapping Ground Deformations and Infrastructure Instability. *In Engineering Geology for Society and Territory –Vol. 2, Springer International Publishing*, 399-403, 2015.
5. Crosetto, M., Monserrat, O., Cuevas-González, M., Devanthéry, N., Luzi, G., Crippa, B. Measuring thermal expansion using X-band persistent scatterer interferometry. *ISPRS J.*, 2015. 100, 84-91.
6. Tomás, R., Márquez, Y., Lopez-Sanchez, J.M., Delgado, J., Blanco, P., Mallorquí, J.J., Martínez, M., Herrera, M., Mulas, J. Mapping ground subsidence induced by aquifer overexploitation using advanced Differential SAR interferometry: Vega Media of the Segura river (SE Spain) case study, *Remote Sensing of Environment*, 2005. 98, 269–283.
7. Bell, J.W., Amelung, F., Ferretti, A., Bianchi, M., Novali, F. Permanent scatterer InSAR reveals seasonal and longterm aquifer-system response to groundwater pumping and artificial recharge, *Water Resour. Res.*, 2008. 44, W02407.

8. Heleno, S.I.N., Oliveira, L.G.S., Henriques, M.J., Falcão, A.P., Lima, J.N.P., Cooksley, G., Ferretti, A., Fonseca, A.M., Lobo- Ferreira, J.P., Fonseca, J.F.B.D. Persistent Scatterers Interferometry detects and measures ground subsidente in Lisbon. *Remote Sensing of Environment*, 2011. 115, 2152–2167.
9. Herrera, G., Tomás, R., López-Sánchez, J.M., Delgado, J., Mallorquí, J.J., Duque, S., Mulas, J. Advanced DInSAR analysis on mining areas: La Union case study (Murcia, SE Spain). *Engineering Geology*, 2007. 90(3), 148-159.
10. Farina, P., Colombo, D., Fumagalli, A., Marks, F., Moretti, S. Permanent Scatterers for landslide investigations: outcomes from the ESA-SLAM project. *Engineering Geology*, 2006. 88(3), 200-217.
11. Tofani, V., Raspini, F., Catani, F., Casagli, N. Persistent Scatterer Interferometry (PSI) technique for landslide characterization and monitoring. *Remote Sensing*, 2013. 5(3), 1045-1065.
12. Notti, D., Davalillo, J.C., Herrera, G., Mora, O. Assessment of the performance of X-band satellite radar data for landslide mapping and monitoring Upper Tena Valley case study. *Nat Hazards Earth Syst Sci*, 2010. 10, 1865-1875.
13. Barra, A., Monserrat, O., Mazzanti, P., Esposito, C., Crosetto, M., Scarascia Mugnozza, G. First insights on the potential of Sentinel-1 for landslides detection. *Geomatics, Natural Hazards and Risk*, 2016. 1-10.
14. Bürgmann, R., Hilley, G., Ferretti, A., Novali, F. Resolving vertical tectonics in the San Francisco Bay Area from permanent scatterer InSAR and GPS analysis. *Geology*, 2006. 34(3), 221-224.
15. Funning, G. J., Bürgmann, R., Ferretti, A., Novali, F., Fumagalli, A. Creep on the Rodgers Creek fault, northern San Francisco Bay area from a 10 year PS‐InSAR dataset. *Geophysical Research Letters*, 2007. 34(19).
16. Reale, D., Nitti, D.O., Peduto, D., Nutricato, R., Bovenga, F., Fornaro, G. Postseismic deformation monitoring with the COSMO/SKYMED constellation. *IEEE Geosci. Remote Sens. Letters*, 2011. 8(4), 696-700.
17. Hooper, A., Pedersen, R., Sigmundsson, F. Constraints on magma intrusion at Eyjafjallajökull and Katla volcanoes in Iceland, from time series SAR interferometry. *The VOLUME Project–Volcanoes: Understanding Subsurface Mass Movement. Dublin: University College*, 2009. 13-24.
18. Ferretti, A., Prati, C. and Rocca, F. Nonlinear subsidence rate estimation using permanent scatterers in differential SAR interferometry. *IEEE TGRS*, 2000. 38(5), 2202–2212.
19. Ferretti, A., Prati, C., and Rocca, F. Permanent scatterers in SAR interferometry. *IEEE TGRS*, 2001. 39(1), 8–20.
20. Berardino, P., Fornaro, G., Lanari, R., and Sansosti, E. A new algorithm for surface deformation monitoring based on small baseline differential SAR interferograms. *IEEE TGRS*, 2002. 40(11), 2375–2383.
21. Lanari, R., Mora, O., Manunta, M., Mallorqui, J.J., Berardino, P., and Sansosti, E. A small-baseline approach for investigating deformations on full-resolution differential SAR interferograms. *IEEE TGRS*, 2004. 42(7), 1377– 1386.
22. Mora, O., Mallorquí, J.J., and Broquetas, A. Linear and nonlinear terrain deformation maps from a reduced set of interferometric SAR images *IEEE TGRS*, 2003. 41(10), 2243–2253.
23. Hooper, A., Zebker, H., Segall, P., and Kampes, B. A new method for measuring deformation on volcanoes and other natural terrains using InSAR persistent scatterers. *Geophysical Research Letters*, 2004. 31, 23.
24. Crosetto, M., Monserrat, O., Cuevas, M., Crippa, B. Spaceborne Differential SAR Interferometry: Data Analysis Tools for Deformation Measurement. *Remote Sensing*, 2011. 3(2), 305-318.
25. Monserrat, O.; Crosetto, M.; Cuevas, M.; Crippa, B. The thermal expansion component of Persistent Scatterer Interferometry observations. *IEEE Geosci. Remote Sens. Lett.*, 2011. 8, 864–868.
26. Hanssen, R. Radar Interferometry. Kluwer Academic Publishers, Dordrecht, The Netherlands, 2001.
27. Yague-Martinez, N., Prats-Iraola, P., Rodriguez Gonzalez, F., Brcic, R., Shau, R., Geudtner, D., Eineder, M., Bamler, R. Interferometric Processing of Sentinel-1 TOPS Data. *IEEE TGRS*, 2016. 54(4), 2220-2234.
28. Prats-Iraola, P., Scheiber, R., Marotti, L., Wollstadt, S., Reigber, A. TOPS interferometry with TerraSAR-X. *IEEE TGRS*, 2012. 50 (8), 3179–3188.
29. Scheiber, R., Moreira, A. Coregistration of interferometric SAR images using spectral diversity. *IEEE TGRS*, 2000. 38 (5), 2179–2191.
30. Devanthéry, N., Crosetto, M., Monserrat, O., Cuevas-González, M., and Crippa, B. An approach to Persistent Scatterer Interferometry. *Remote Sensing*, 2014. 6(7), 6662-6679.
31. Costantini, M.: A novel phase unwrapping method based on network programming. *IEEE TGRS*, 1998. 36, 813–821.
32. Costantini, M., Farina, A., Zirilli, F.: A fast phase unwrapping algorithm for SAR interferometry. *IEEE TGRS*, 1999. 37, 452–460.
33. Baarda, W. A Testing Procedure for Use in Geodetic Networks. *Kanaalweg 4, Rijkscommissie voor Geodesie: Delft, The Netherlands*, 1968.
34. Björck, Å. Numerical Methods for Least Square Problems. *Siam: Philadelphia*, PA, USA, 1996.
35. Förstner, W. Reliability, gross error detection and self-calibration. *ISPRS Commission III Tutorial on Statistical Concepts for Quality Control. ISPRS Int. Arch. Photogramm.*, 1986, 26, 1–34.